ORIGINAL ARTICLE

Monica Lupi · Paolo Cappella · Giada Matera ·
Claudia Natoli · Paolo Ubezio

Interpreting cell cycle effects of drugs: the case of melphalan

Abstract Multiple effects usually occur in the cell cycle, during and after the exposure to a drug, while treated cells flowing through the cycle encounter G_1, S and G_2M checkpoints. We developed a simulation tool connecting the microscopic level of the cellular response in G_1, S and G_2M with the experimental data of growth inhibition and flow cytometry. We found that multiple—often not intuitive—combinations of cytostatic and cytotoxic effects can be in keeping with the observations. This multiplicity of interpretation can be strongly reduced by considering together data with different methods, ideally reaching a reconstruction of the underlying cell cycle perturbations. Here, we propose an experimental plan including a time course of DNA flow cytometry and absolute cell count measurements with several drug concentrations and a limited number of flow cytometric DNA-Bromodeoxyuridine and TUNEL analyses, coupled with computer simulation. We showed its use in the attempt to define the complete time course of the effects of melphalan on three cancer cell lines. After drug treatment, each subset of cells experienced blocks and lethality in all phases of the cell cycle, but the dynamics was different, the differences being strongly dose-dependent. Our approach allows a better appreciation of the complexity of the cell cycle phenomena associated with drug treatment. It is expected that such level of understanding of the time- and dose-dependence of the cytostatic and cytotoxic effects of a drug might support rational therapeutic design.

M. Lupi · P. Cappella · G. Matera
C. Natoli · P. Ubezio (✉)
Biophysics Unit, Laboratory of Cancer Pharmacology,
Department of Oncology, Istituto di Ricerche
Farmacologiche ''Mario Negri'', Via Eritrea 62,
20157, Milano, Italy
E-mail: ubezio@marionegri.it
Tel.: +39-02-39014438
Fax: +39-02-3546277

Introduction

Alkylating agents are a major class of anticancer drugs with established clinical activity against a broad spectrum of human malignancies [18, 19]. They act by forming a highly reactive carbonium ion that can react with negatively charged electron-rich nucleophilic sites on biological molecules, adding an alkyl group at either oxygen, nitrogen, phosphorous or sulphur atoms. DNA alkylation is commonly considered the main cause of cell toxicity and death, leading to the production of DNA–DNA inter- or intrastrand cross-links and DNA–protein cross-links [13, 17]. Differences in the efficiency of repair of DNA damage and the metabolic inactivation by protecting agents like glutathione partly explain the varying cell sensitivity to these drugs [16, 20].

The nitrogen mustard derivative L-phenylalanine mustard (melphalan, L-PAM) is a typical representative of this class of drugs. L-PAM, like the other alkylating agents, is considered a fairly non cycle-specific drug, as it is active even against resting cells [21]. Results with synchronised cells indicate that G_1 is the most sensitive phase to most alkylating agents, including L-PAM [14]. Mid to late S is the most resistant phase of the cell cycle, while the most affected phase with respect to cell progression (cytostatic effect) appears to be G_2M. DNA flow cytometry shows asynchronous cell populations accumulated in G_2M after treatment with several alkylating agents. Both the magnitude and the duration of G_2M block depend on the phase at treatment [1]. Erba et al. [8] reported a flow cytometric study of cell cycle effects of L-PAM on an ovarian cancer cell line. DNA histograms and bromodeoxyuridine (BrdUrd) dot plots indicate a slowing down of cells through S phase and a progressive cell accumulation in G_2M.

However, all these studies only tested one or two concentrations of the drug and interpretation of the cell

cycle distribution data could be difficult because the flow cytometric percentages reflect a superimposition of the effects of cell cycle block and cell loss. On the other hand, the individual cell's response to treatment might vary because of inter-cell differences in drug uptake and intracellular content of different molecules.

We present a mixed computational-experimental approach that can support the interpretation of data obtained with classical experimental methods for in vitro drug testing.

Our approach [12] enabled to obtain a complete analysis of L-PAM's effects on three cancer cell lines growing exponentially in vitro. We deciphered the experimental data (flow cytometric percentages and absolute cell number) by a mathematical model in terms of the underlying phenomena of inhibition of DNA synthesis, G_1 and G_2M block, death or recycling, as they superimpose on the "physiological" cell cycle progression.

By fitting the time-courses for several drug concentrations, we obtained a "scenario" that provides an overall picture of a cell population's response to the drug challenge. The "scenario" is a set of parameters (called "effect descriptors"): probabilities of G_1 and G_2M block, S-phase delay, recycling and death rate that quantify the activity of a specific molecular network, with its time- and dose-dependence. The specificity of each descriptor enables us to distinguish the cytostatic and cytotoxic effects of the drugs. In addition, the probabilistic measure of each descriptor takes inter-cell variability into account.

Materials and methods

Cell culture and drug treatment

We studied the effects of L-PAM (Sigma, St. Louis, MO, USA) using two ovarian cancer cell lines, IGROV1 and A2780, and a colon carcinoma cell line HCT-116, maintained as monolayers in T-25 cm^2 tissue culture flasks (Iwaki, Bibby Sterilin, Staffordshire, UK). The culture medium of IGROV1 and A2780 consisted of RPMI-1640 medium (Sigma) with 10% foetal bovine serum (Euroclone, CELBIO, Milano, Italy) and 1% L-glutamine (Sigma). HCT-116 was cultured in IMDM (Cambrex, Verviers, Belgium) with 10% foetal bovine serum (Euroclone) and 1% L-glutamine (Sigma). Culture was maintained in an incubator with 5% CO_2 in air, at 37°C and 96% relative humidity. Exponentially growing cells were treated for 1 h with different drug concentrations (3, 10, 30, 50, 100, 300 μM). After treatment, the cells were washed twice with warm PBS and left in drug-free medium for specified times, in our case 0, 6, 24, 48 and 72 h. At each time, cells were detached using 1 ml 0.05% trypsin-0.02% EDTA (Cambrex) in PBS, counted with a Coulter Counter ZM (Coulter Electronics, Harpenden, UK), then fixed in cold 70% ethanol.

Flow cytometric analysis

DNA analysis was done on cells fixed at different times after treatment. Short and long-term perturbations were investigated by BrdUrd pulse-and-chase analysis. BrdUrd (Sigma) replaces thymidine during DNA synthesis, catching cells that are in S phase during the pulse. The cells were labelled with 30 μM BrdUrd for 15 min before the end of the 1 h treatment. The BrdUrd pulse-and-chase 6 h after the treatment detects cell movement through the S phase and the outflow of unlabeled G_1 and G_2M cells; we considered the pulse-and-chase 72 h after treatment as an indication of the preferential cytotoxicity of the drug.

Monoparametric staining of DNA content

About $1×10^6$ fixed cells were washed with cold PBS and re-suspended in 1 ml of 25 μg/ml PI (Calbiochem, Darmstad, Germany) in PBS plus 25 μl of 1 mg/ml RNAse (Sigma) in H_2O. The samples were measured with a FACS Calibur (Becton Dickinson, San Jose, CA, USA) flow cytometer after about 2 h incubation at room temperature in the dark.

Two-parameter flow cytometry analysis: DNA content and BrdUrd incorporation

About $2×10^6$ fixed cells were washed with PBS and re-suspended in 3 N HCl for 30 min. After washing with 0.1 M $Na_2B_4O_7$, pH 8.5, to stop acid depurination, the cells were re-suspended with 180 μl 0.5% Tween 20 (Sigma) with 1% normal goat serum (NGS) (Dako, Glostrup, Denmark) in PBS. After this, 20 μl anti-BrdUrd monoclonal antibody (Becton Dickinson) was added and the mixture was incubated for 1 h at room temperature. After washing with PBS, cells were incubated for 1 h with fluorescein (FITC)-conjugated affinity pure F(ab')2 fragment goat antimouse IgG (Jackson, West Grove, PA, USA) diluted 1:50 in PBS with 0.5% Tween 20 and 1% NGS. After incubation with antibody, cells were centrifuged, re-suspended in 2.5 μg/ml PI in PBS plus 25 μl of 1 mg/ml RNAse in H_2O, incubated overnight and analysed.

In the case of direct BrdUrd immunostaining, we added 20 μl anti-BrdUrd FITC (Becton Dickinson) at the cells re-suspended in 180 μl 0.5% Tween 20. After 1 h incubation, the cells were washed with PBS and re-suspended in 2.5 μg/ml PI in PBS plus 25 μl of 1 mg/ml RNAse in H_2O, incubated overnight and analysed.

Two-parameter flow cytometry analysis: DNA content and FITC-conjugated dUTP

DNA fragmentation was detected by the TdT-mediated dUTP nick end labeling technique (TUNEL), which uses terminal deoxynucleotidyl transferase (TdT) to catalyse

the binding of FITC-conjugated dUTP to DNA strand breaks. This technique detects DNA fragmentation induced during apoptosis. 2×10^6 fixed cells were washed in PBS and permeabilized for 2 min on ice in 0.1% Triton X-100, 0.1% sodium citrate. The cells were washed, re-suspended in 50 μl of TUNEL reaction mixture (Roche, Mannheim, Germany) containing dUTP-FITC and TdT, and incubated for 90 min at 37°C in the dark. After that, the samples were washed and re-suspended in 1 μg/ml PI plus 25 μl of 1 mg/ml RNAse in H_2O and incubated overnight at 4°C.

Computer simulation of cell population growth and drug effects

The computer program has already been described in detail elsewhere [15]. It is an important tool for quantitatively combining all the experimental data. Starting from the cell cycle distribution at a given time, this model predicts cell cycle flux. It reproduces the unperturbed growth of a cell population and its response to several drug concentrations, by constructing a complete and coherent kinetic scenario based on a quantitative estimate of the time-and dose-dependence of the probabilities of cell arrest and killing.

Unperturbed growth

To simulate the unperturbed growth of each cell line, we adopted the following parameters:

IGROV1 : $T_{G1} = 3.0\,\text{h}; CV_{G1} = 50\%; T_S = 8.7\,\text{h}; CV_S = 10\%; T_{G2M} = 3.1\,\text{h}; CV_{G2M} = 10\%$

A2780 : $T_{G1} = 6.4\,\text{h}; CV_{G1} = 50\%; T_S = 9.1\,\text{h}; CV_S = 20\%; T_{G2M} = 3.4\,\text{h}; CV_{G2M} = 25\%$

HCT $-$ 116 : $T_{G1} = 1.8\,\text{h}; CV_{G1} = 20\%; T_S = 9.5\,\text{h}; CV_S = 5\%; T_{G2M} = 3.2\,\text{h}; CV_{G2M} = 20\%,$

where T_{G1}, T_S, T_{G2M} and CV_{G1}, CV_S, CV_{G2M} are respectively the mean and the coefficient of variation of the transit times in the cell cycle phases.

As cells were treated while in exponential growth, we adopted the asynchronous cell distribution (where cell percentages in every phase are constant over time) as starting distribution.

Drug effects

To simulate all possible cell cycle perturbations, a set of additional parameters ("effect descriptors") was devised, all associated with cell cycle perturbations with a true biological significance:

– "Delay" rate: this is the proportion of cells whose progression inside S phase is inhibited at each step, resulting in a longer mean transit time. The value of the parameter is equivalent to the fractional reduction of the mean DNA synthesis rate. The extreme situation (delay rate = 1) indicates complete cell "freezing" in S phase.
– "Block" probability: this is the proportion of cells entering a block in G_1 or G_2M, instead of proceeding to the next phase. In other words, "Block" represents the probability of being intercepted by a checkpoint and blocked there. Blocked cells may subsequently either re-enter the cycle or die in the block, depending on the next two parameters.
– "Recycling" rate: this is the proportion of blocked cells re-entering the cycle at each time step. It is indicative of recovery in cells blocked at a checkpoint.
– "Death" rate: this is the proportion of cells removed from a group at each time step. Independent rates can be applied to cycling, blocked or delayed cells in a phase.

The death and recycling rates are expressed in terms of the corresponding percentage of cells that would die or recycle in a group of blocked cells in the interval of interest.

Output data

While a set of values for the parameters describing drug effects (the "scenario" under evaluation) is given as input, the simulation program as output then gives the time course of several measurable quantities consequent to this scenario. These values are compared directly with the experimental data:

– Total number of cells, reproducing the growth curve.
– Percentages of cells in the G_1, S and G_2M phases.
– Output of BrdUrd experiments: percentages of G_1, S, G_2M BrdUrd unlabeled cells; percentages of "undivided" and "divided" BrdUrd-positive cells (i.e. BrdUrd-labeled cells still in the S and G_2M phases of their first simulated cycle, and in the G_1 phase of their second simulated cycle); total percentage of BrdUrd-positive cells.

Optimisation

During the simulation, hundreds of sets of input parameters are tested by a trial-and-error procedure. As the experimental precision of flow cytometric percentages is about 3% and cell counts 20%, the fitting was considered satisfactory when all experimental data were reproduced with the same precision. Using a principle of parsimony, we started trying to reproduce the data with a few parameters, as suggested by the interpretation of flow cytometric data and adding progressively new parameters until we obtained a satisfactory reproduction of all available data. The data of each drug concentration were initially fitted independently, finding a small number of scenarios coherent with data. Then, the

dose-dependence of each parameter was considered, allowing the exclusion of some biologically inconsistent scenarios that forecasted a decrease of overall blocks and cell loss when drug concentration increases.

The parameters were taken as constant in the intervals between successive experimental data (i.e. 0–6, 6–24, 24–48 and 48–72 h). The resulting values for "Block", "Recycling" and "Death" should be considered as descriptions of average effects in those intervals. The adopted time intervals are a compromise between feasibility of the experiment and necessity to have an estimate of the time-course.

We found that the hypothesis of the time-dependence of the parameters is necessary to fit the data but any detail of that time-dependence inside subsequent data points was not necessary and would not be demonstrable.

Sensitivity

To study the sensitivity of each parameter in our model we took into account every non-zero parameter in the best scenario reproducing the experimental data and changed them, one by one, in a wide range.

For each parameter, a confidence band was constructed including all values enabling to simulate the data with a 3% tolerance for flow cytometric percentages or 20% for cell counts.

Results

Exponentially growing IGROV1 cells were treated for 1 h with 3, 10, 30, 50, 100, 300 µM of L-PAM. Then we measured the following quantities related to the cell kinetics: overall (absolute) cell number, flow cytometric DNA histograms, biparametric DNA-BrdUrd flow cytometric histograms using the pulse-chase protocol.

Figure 1 shows the growth curves after treatment. The cells treated with 3 µM L-PAM grew like controls
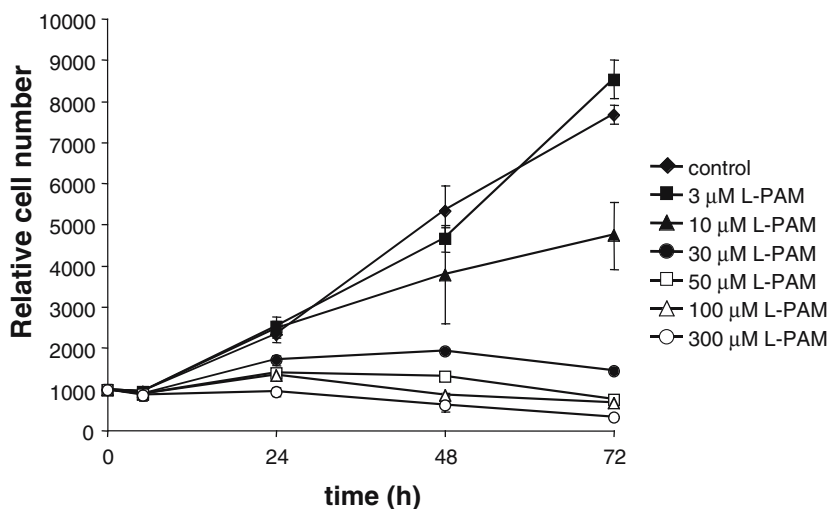
and the number of cells treated with 10 µM decreased only after 48 h. From 30 to 300 µM the behaviour of the cells was very similar, the number remaining almost constant until 48 h and starting to decrease between 48 and 72 h.

Flow cytometric DNA histograms of control and treated samples are shown in Fig. 2. Differences between the treated samples and the control were detectable only 24 h after treatment when the cells treated with 10, 30, 50 and 100 µM L-PAM accumulated in G_2M phase. The duration of this block was apparently dose-dependent, and for the samples treated with 50 µM and higher concentrations high levels of G_2M cells were present up to the end of observation (72 h). At 48 h, the cells treated with the highest concentrations (100 and 300 µM) contained a large amount of debris.

Short-term effects of L-PAM were evaluated by a pulse-chase experiment. Cells were exposed to BrdUrd in the last 15 min of treatment, allowing DNA-synthesising cells to incorporate BrdUrd, becoming "BrdUrd-positive", and were collected 6 h later. The resulting biparametric DNA-BrdUrd plots, in Fig. 3a, indicate the movement of the cells in the cycle in the first 6 h after treatment. In untreated and in 3-µM treated samples BrdUrd-positive cells that occupied S phase at 0 h were distributed in late S, G_2M and G_1 phases at 6 h. In samples treated, with concentrations higher than 3 µM, the percentage of BrdUrd-positive cells in G_1 ($G_1 +$) was lower. This was probably caused more by a block in G_2M than by a delay in S phase, because the movement of BrdUrd-positive cells towards G_2M was visibly reduced only for samples treated with 300 µM L-PAM.

Because more than one scenario of cytotoxic and cytostatic effects might explain the previous data, a BrdUrd pulse-chase experiment was subsequently done, collecting cells 72 h after treatment and BrdUrd pulse. The BrdUrd dot plots shown in Fig. 3b showed that more BrdUrd-positive than BrdUrd-negative cells survived 72 h after treatment. This difference decreased as higher drug concentrations were used. The samples treated with 10 or 50 µM L-PAM presented about 80%
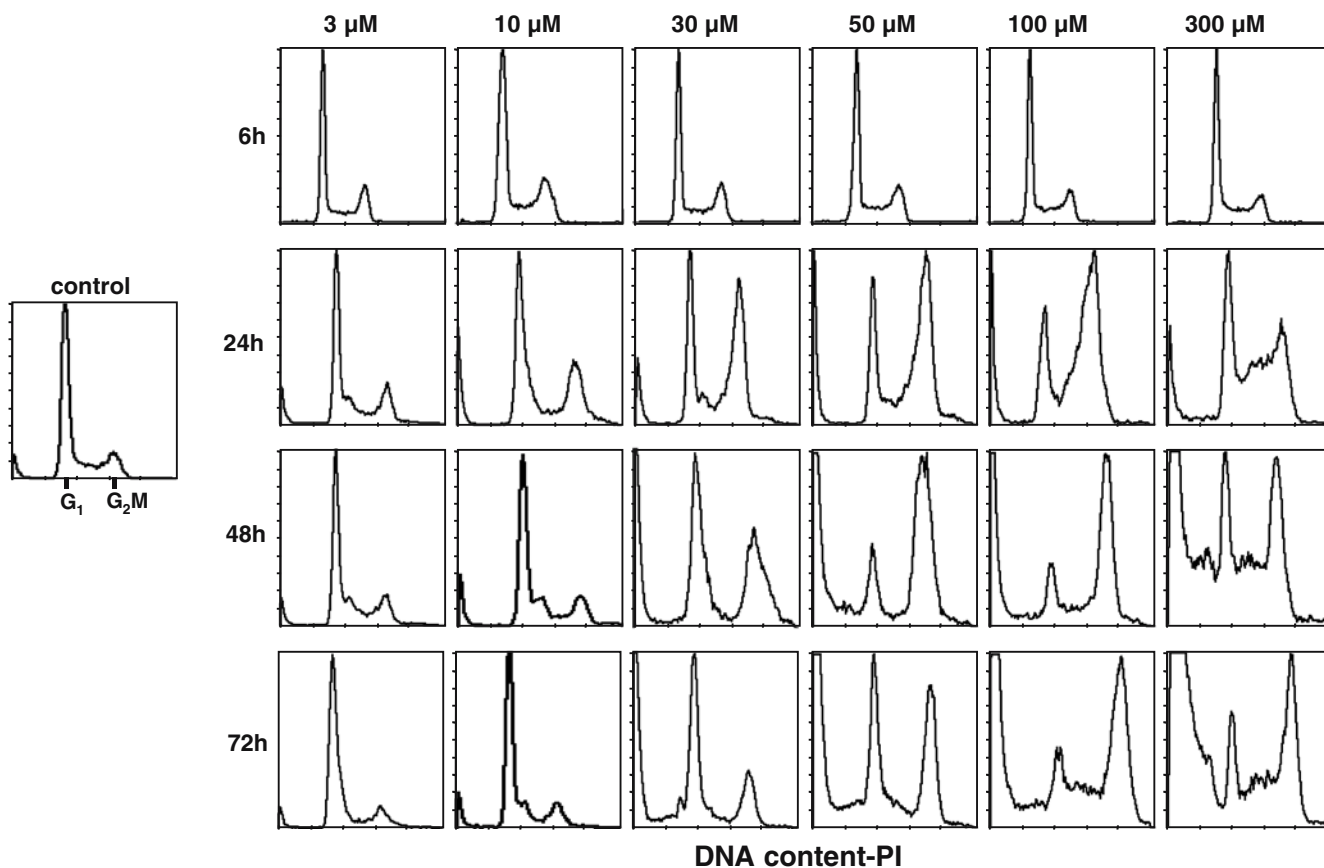
Fig. 1 Growth curves of IGROV1 cells after 3, 10, 30, 50, 100, 300 µM L-PAM for 1 h, measured by Coulter Counter. Each point is an average of at least three replicate flasks

Fig. 2 Time course of DNA histograms after 3, 10, 30, 50, 100, 300 μM L-PAM for 1 h. DNA corresponding to G_1 and G_2M cells is indicated. Persistent accumulation in the G_2M peak is particularly evident in the 50, 100 and 300 μM histograms, while a large amount of debris (in the region to the left of G_1 peak) is present at 48 h and 72 h in the cells treated with 300 μM L-PAM

of BrdUrd-positive cells after 72 h, while after 300 μM L-PAM there was only about 50% of BrdUrd-positive cells.

Another qualitative picture of the drug effects can be obtained from Fig. 4, where the TUNEL technique confirmed the cell killing in samples treated with the highest drug concentrations. The cells treated with 300 μM L-PAM showed a substantial percentage of dUTP-FITC-positive cells from 24 h; 50 and 100 μM L-PAM had cytotoxic effects after 48 h.

Considering the results of the additional experiments, we selected a scenario coherent with all available data, taking into account as quantitative data of the flow cytometric percentages from DNA histograms, BrdUrd dot-plots and cell count, and as qualitative data the information from the dUTP-assay. Figure 5 shows the values of the parameters constituting the scenario. In each panel, the colour of a square indicates the parameter strength in a specific interval of time (column) and at a specific L-PAM concentration (row). The parameters are indicated as non-detectable (ND) when there were too few cells in a specific cell cycle phase to establish their value.

Events in G_1 phase (Fig. 5a)

The molecular controls of G_1 phase act during and immediately after treatment on BrdUrd-negative cells. However, the blocking activity was not strong: 5–20% for 30–100 μM, or 20–40% for the highest concentrations, of BrdUrd-negative cells remained blocked in this phase immediately after treatment (upper right panel). The duration of the block is dose dependent: it ended 6 h after treatment with 30 μM, 24 h with 30 and 100 μM, 48 h with 300 μM, only at the highest concentration the same blocking activity was observed also in BrdUrd-positive cells (upper left panel).

Cells treated with at least 50 μM and blocked in G_1 died in this phase after 24 h (lower panels). The highest concentration was cytotoxic for both BrdUrd-positive and BrdUrd-negative cells blocked in this phase (lower left panel). The recycling rate for cells intercepted by this checkpoint was negligible (not shown).

Events in S phase (Fig. 5b)

BrdUrd-positive cells that were treated with at least 30 μM L-PAM immediately reduced their DNA synthesis rate. This reduction was either constant or, for the highest concentrations, increased with time, reaching 80–100% between 24 and 72 h (top left panel). The behaviour of BrdUrd-negative cells was very similar
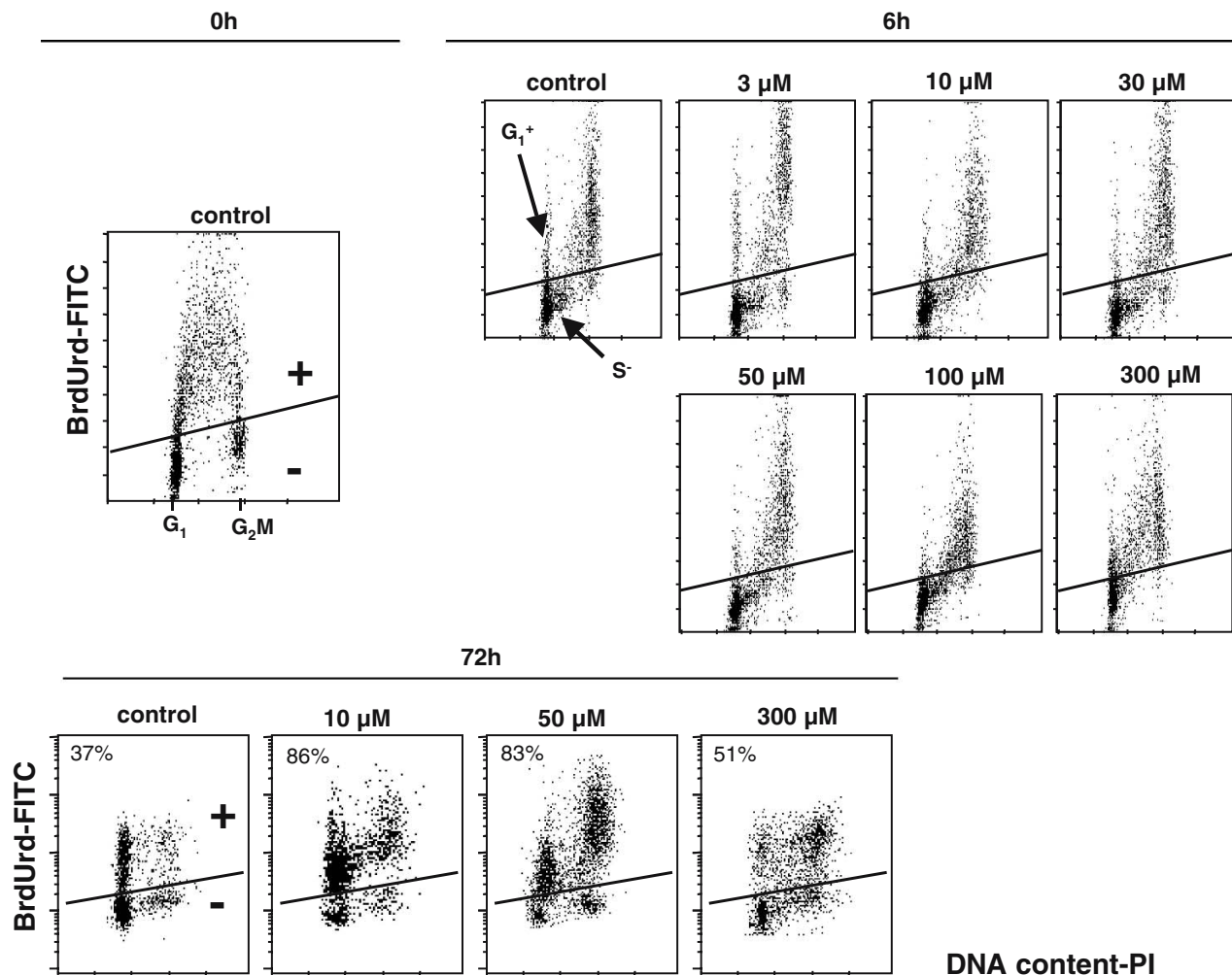
Fig. 3 Biparametric PI-fluorescence (DNA content) and FITC-fluorescence (BrdUrd content) plots. Cells incorporated BrdUrd 15 min before the end of the 1 h-treatment and were harvested after 6 h (**a**) and 72 h (**b**) (BrdUrd pulse-chase). Cells were considered BrdUrd-positive (in the S phase at the time of treatment, 0 h) when detected above the line, drawn on the basis of the fluorescence level of G_1 and G_2M subpopulations of 0 h controls. BrdUrd-positive cells with G_1 DNA content (G_1 +) at 6 h were born from mitosis of cells in S phase at the time of treatment. G_1 BrdUrd-positive cells are present in the control and in samples treated with the lowest concentration of L-PAM. The percentage of G_1 + cells is lower in samples treated with L-PAM concentrations higher than 3 μM. In the BrdUrd pulse-chase experiment 72 h after treatment the percentage of BrdUrd-positive cells is higher than that of BrdUrd-negative ones, this difference decreasing as the drug concentration increases. The percentage of BrdUrd-positive cell is reported on the graphs. Six-hour samples were detected by direct immunostaining and are thus represented with a linear BrdUrd scale; 72 h samples were detected by indirect immunostaining and are represented with a logarithmic BrdUrd scale

though the effects were stronger (top right panel). At 24 h after treatment, both BrdUrd-positive and BrdUrd-negative cells started to die in this phase. Again, this effect was stronger for BrdUrd-negative cells, with 60–80% of cells traversing the S phase in 24 h dying

(L-PAM >10 μM), compared to 20–40% of BrdUrd-positive cells (lower panels).

Events in G_2M phase (Fig. 5c)

The block in G_2M was stronger for cells treated in G_1 and G_2M phase (BrdUrd-negative, top right panel) than for cells treated in S phase (BrdUrd-positive, top left panel). At the lowest concentrations (3 and 10 μM), the block ended 6 h after treatment for both BrdUrd-positive and BrdUrd-negative cells, while it persisted until 72 h for the samples treated with higher concentrations. For BrdUrd-negative cells the intensity of G_2M blocking activity increased after 6 h and 60–80% of cells were intercepted by this checkpoint in the samples treated with 50, 100 and 300 μM L-PAM. As shown in the lower panels, cells blocked in G_2M phase started to die 24 h after treatment, except for those treated with 3 and 10 μM, where this effect was not detectable. After 6 h, 80–100% of cells treated with the highest concentration and blocked in this phase died in each interval.

The final scenario shown in Fig. 5 allowed the reproduction of all the data within the experimental

Fig. 4 Biparametric PI-fluorescence (DNA content) and FITC-fluorescence (dUTP content). Cells with DNA fragmentation induced during apoptosis are dUTP-positive (above the straight line). For the analysis, only cells with a DNA content higher than 1/10 of G_1 were considered
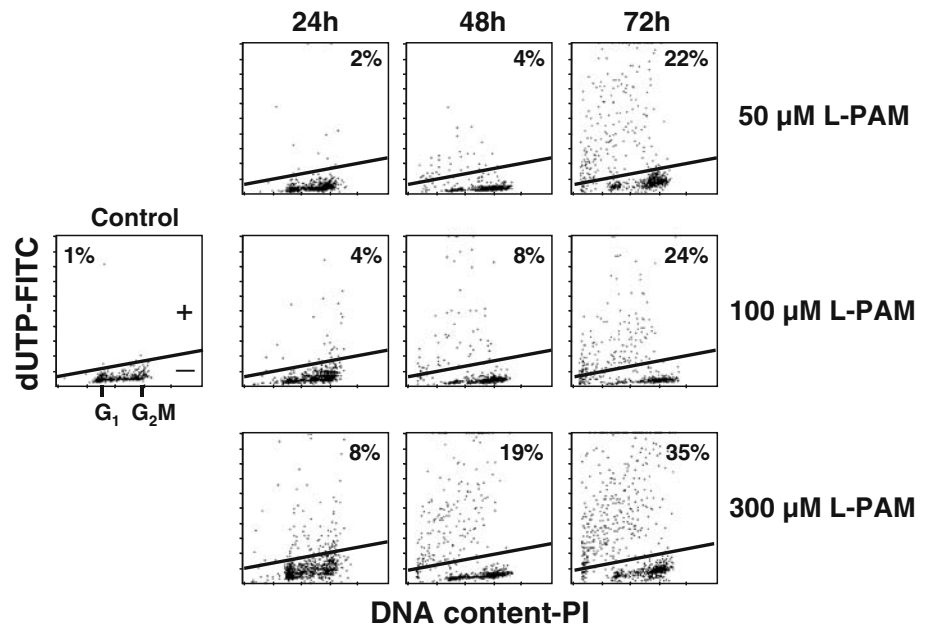
precision, i.e. 3% for flow cytometric percentages and 20% for cell counts. However, a further level of evaluation is necessary to measure the uncertainty of the parameters estimation (sensitivity analysis). For this purpose, we started from the scenario obtained and we varied each parameter on its own to determine the impact of this variation on the output. Figure 6 presents the time courses of each parameter obtained with our final simulation (shown as a continuous line) and the results from the study of the sensitivity. The filled area indicates the range of values for each parameter within which the simulation reproduced the data within their experimental error (see Materials and methods). A wide band means that a given parameter, at the specified time and concentration, is irrelevant for the data, while a narrow band means that the estimate is robust and the prediction of the observed data would be lost with small changes to the assumed value.

The parameter of G_1 blocking activity was very sensitive, excluding the presence of strong activity but indicating that a weak activity should necessarily be included at ≥ 30 μM L-PAM (Fig. 6a). The G_1 blocking activity of BrdUrd-positive cells was irrelevant for the outcome between 0 and 6 h, because there was no time for these cells to reach the G_1–S transition, where the block would be detectable. Sensitivity analysis showed that in most cases, the parameters of S phase delay (Fig. 6b, first and second row) and G_2M blocking activity (Fig. 6c, first and second row) were precisely estimated, confirming in both cases the increase in drug effects with time and drug concentration.

The parameters connected with the loss of G_1 and G_2M blocked cells obviously became sensitive only when a subpopulation of blocked cells was no longer negligible, and this happened a long time after treatment or with high drug concentrations (Fig. 6a, c, bottom row).

In these instances, the need to include loss from both G_1 and G_2M was confirmed by the sensitivity analysis. Particularly, in order to maintain the correspondence with the data, a fairly high loss needs to be included among BrdUrd-negative blocked G_1 cells from 100 μM (while this effect could not be detected with 50 μM) but only at 300 μM among BrdUrd-positive G_1 cells. Lethality among G_2M blocked cells was proved after 24 h at ≥ 30 μM in both BrdUrd-positive and BrdUrd-negative subpopulations, with similar strength, while lethality in S phase was demonstrated at 48 h even at 10 μM and at 24 h from 30 μM (Fig. 6b, bottom row).

After evaluating the precision of the selected scenario, we wanted to exclude the possibility that different combinations of the parameters' values would enable to reproduce the data and to suggest a different—biologically coherent—dynamics of the cell cycle response.

Alternative scenarios were searched varying systematically all parameters together. By testing about 100,000 combinations of parameters' values for each drug concentration, we were able to identify only a few variants (not much different) to the results shown in Fig. 5. These included recycling at low concentrations, somewhat stronger short-time block in G_1 and G_2M phase, with loss in both cell cycle phases at 100 μM, a stronger short-time delay with loss in S phase and a reduced G_2M loss at 300 μM. Particularly, the recycling rate was compatible with our data and with increased G_2M blocking activity between 6 and 24 h after treatment, whereas at longer times, this parameter became negligible and was replaced by a loss rate (not shown).

We addressed the issue of the reproducibility of the scenario with different cell lines, performing the same analysis on data obtained with another ovarian cancer cell line (A2780) and a colon carcinoma cell line
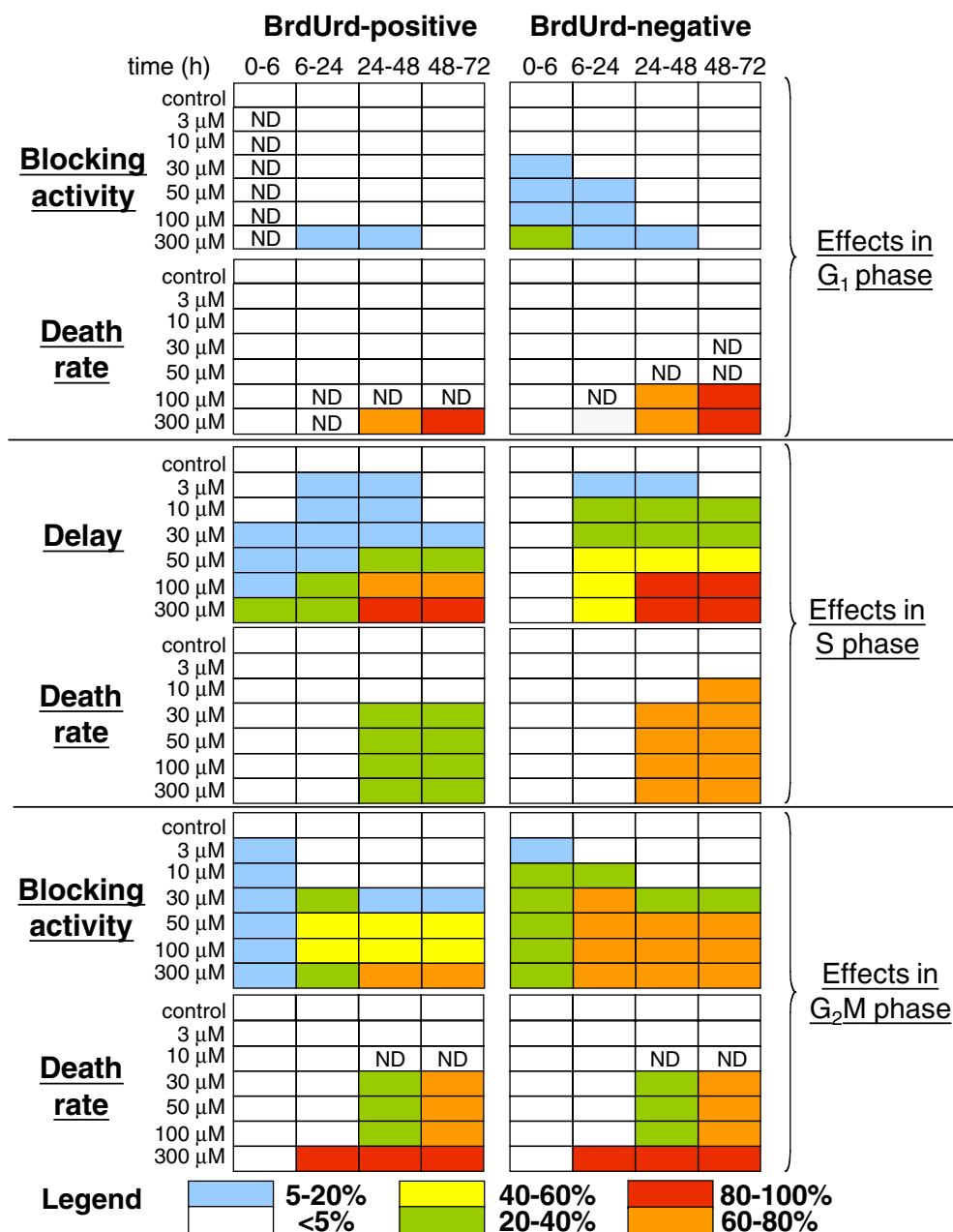
BrdUrd-positive   **BrdUrd-negative**

time (h)   0-6 6-24 24-48 48-72   0-6 6-24 24-48 48-72

Blocking activity (control, 3 μM, 10 μM, 30 μM, 50 μM, 100 μM, 300 μM)

Death rate (control, 3 μM, 10 μM, 30 μM, 50 μM, 100 μM, 300 μM)

} Effects in G_1 phase

Delay (control, 3 μM, 10 μM, 30 μM, 50 μM, 100 μM, 300 μM)

Death rate (control, 3 μM, 10 μM, 30 μM, 50 μM, 100 μM, 300 μM)

} Effects in S phase

Blocking activity (control, 3 μM, 10 μM, 30 μM, 50 μM, 100 μM, 300 μM)

Death rate (control, 3 μM, 10 μM, 30 μM, 50 μM, 100 μM, 300 μM)

} Effects in G_2M phase

Legend   5-20%   40-60%   80-100%   <5%   20-40%   60-80%

Fig. 5 The response scenario for complete reproduction of the experimental data. Blocking activity is the percentage of cells that remain blocked among those traversing G_1 or G_2M in the interval indicated. The death rates are the percentages of cells that die in each interval, within the compartment of G_1 (or G_2M) blocked cells. In the 0–6 h interval the death rate in G_1 or G_2M applies to both blocked and proliferating cells, because they cannot be distinguished. Parameters of irrelevant values are defined as ND (non-detectable). The S-delay rate is equivalent to the percentage reduction of the average DNA synthesis rate

(HCT-116). The scenarios obtained with A2780 and HCT-116 were compared with that of IGROV1 cells.

Figure 7 shows in a synthetic way the measures of the cytostatic effects induced by the drug on three different cell lines, considering together BrdUrd-positive and BrdUrd-negative cells at short (0–24 h) and at long (24–72 h) times after treatment. Overall drug efficacy was not the same for different cell lines: A2780 were about threefold more sensitive than IGROV1 cells to L-PAM treatment, whereas HCT-116 resulted to be more resistant to this drug.

Nevertheless, we obtained similar patterns of response of IGROV1, A2780 and HCT-116 comparing drug concentrations with equivalent efficacy. The low activation of G_1 checkpoint, the presence of a delay in the progression through S phase and a strong G_2M blocking activity were observed in all the cell lines. Main differences were a short-term G_2M block stronger for HCT-116 (Fig. 7, lower left panel) and a stronger delay in S phase for A2780 (Fig. 7, second line panels). The outcome of G_2M block was also different in HCT-116

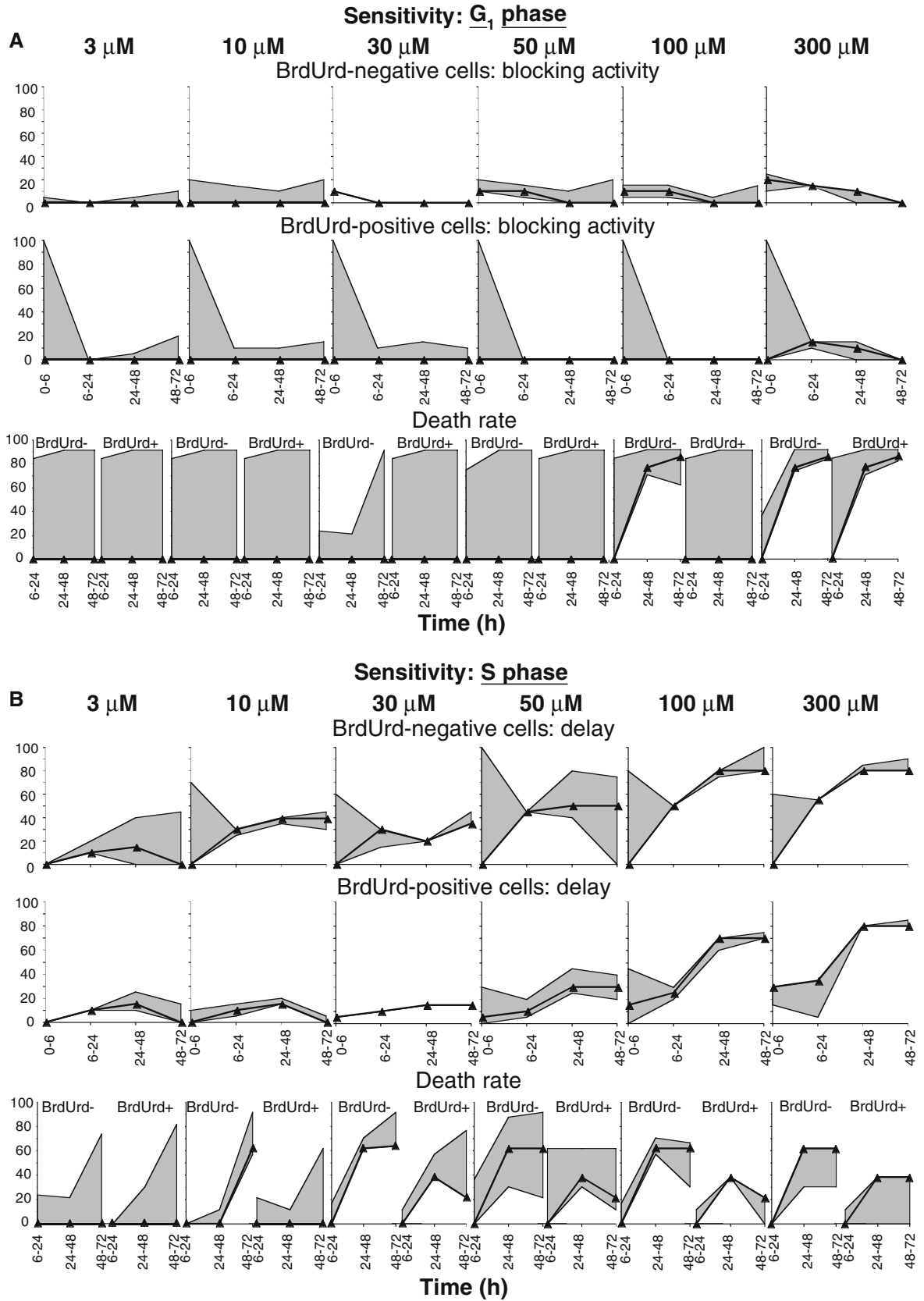## Sensitivity: $\underline{G_1}$ phase

A

Fig. 6 Time courses of the parameters used in the simulation (same units as Fig. 5). The *continuous line* indicates the value of each parameter as obtained in the final simulation and the *filled area* represents the range of values for each parameter within which the simulation remained close to the experimental data
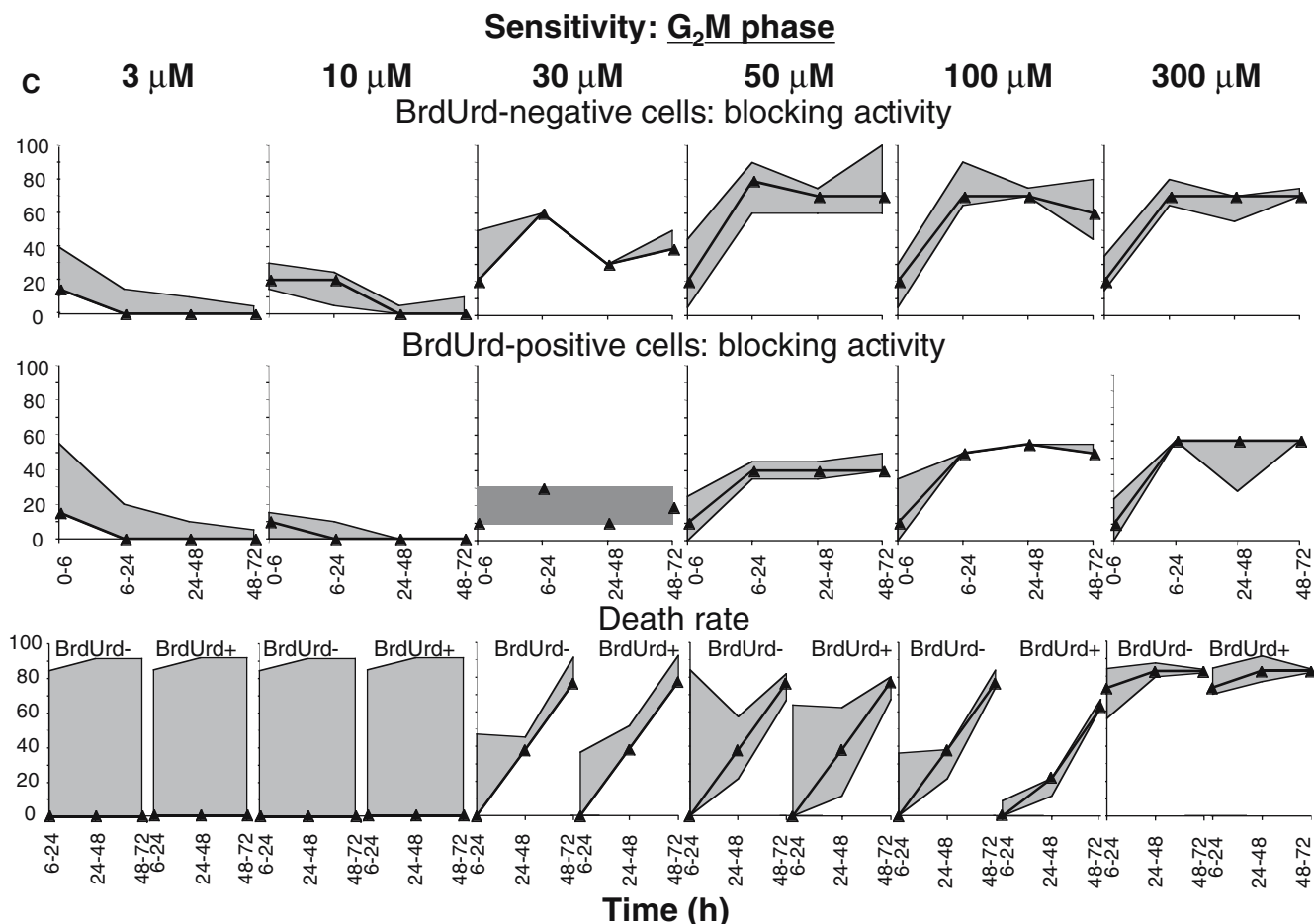
Sensitivity: G₂M phase

Fig. 6 (Contd.)

respect to IGROV1 and A2780 cells, HCT-116 did not die in this phase, even when treated with very high L-PAM concentrations. Moreover, in the samples treated with low drug concentrations, recycling of G₂M-blocked cells could be unambiguously detected in HCT-116 cells (not shown). Some recycling from blocks was also detected for A2780 cells in G₁ (very high concentrations) and in G₂M phase (low concentrations).
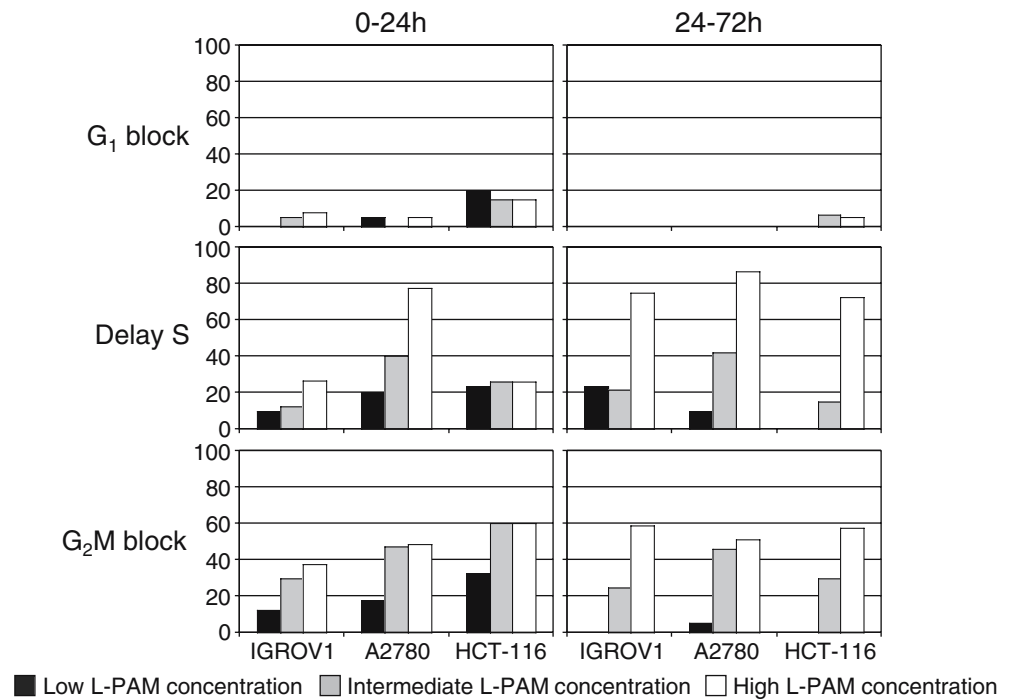
As the final scenario obtained with IGROV1 was confirmed by the sensitivity analysis and by the comparison with the scenarios obtained with other cell lines, its predictions were investigated in detail using the simulation program. This way, we could disclose information on the behaviour and heterogeneity of the cell population that could not be directly measurable from the experimental data. We retrieved from the simulation the percentage of cells blocked in G₁ or in G₂M at each time (Fig. 8) and the total amount of cells dying in the 72 h of observation (Fig. 9). The quantities shown in these two figures allowed the evaluation of the impact of a specific block and killing on the growth of the whole cell population. On the other side, the values in Fig. 5 indicate the average strength of the blocking or killing activity within the cells that reached a specific phase, independently from their number.

Figure 8 shows the total amount of cells blocked in G₁ or in G₂M compared with the percentage of cells in the same phase. Of course, %G₁ and %G₂M directly measured by flow cytometry were unable to distinguish blocked from cycling cells. The percentage of cells blocked in G₁ is non-zero only for the samples treated with concentrations higher than 30 μM and it involves more than 10% of the whole cell population only at the highest concentration (300 μM). The percentage of G₁ blocked cells peaked in the first 24 h (between 10 and 20% of all cells with 300 μM) but it decreased later on, more because of cell loss than because of proliferation of other cells.

At drug concentrations higher than 30 μM the majority of G₂M cells were blocked at 24 h. The percentage of blocked G₂M cells rose until 48 h, then decreased again, more because of cell loss than because of proliferation of other cells. At 24 h, with the highest concentration, G₂M blocked cells were less than G₁ blocked ones.

The percentage of cells lost in 72 h is presented in Fig. 9. Drug concentrations higher than 30 μM had a strong cytotoxic effect, and about 65% of cells died after treatment with 30 μM L-PAM. The pies above the columns give the distribution of cells lost in the different

Fig. 7 Comparison between the cytostatic effects induced by L-PAM on IGROV1, A2780 and HCT-116, as measured by best fit values of G_1 and G_2M block probabilities and S-delay rate (same units as Fig. 5). Each column represents average values of parameters at short (0–24 h) and at long (24–72 h) times after treatment, including both BrdUrd-positive and BrdUrd-negative cells. Drug concentrations: low efficacy (10 µM IGROV1, 3 µM A2780, 30 µM HCT-116), intermediate efficacy (30 µM IGROV1, 10 µM A2780, 100 µM HCT-116), high efficacy (100 µM IGROV1, 30 µM A2780, 300 µM HCT-116)

cell cycle phases. After 10 µM L-PAM the cytotoxic effect was explained by a loss of cells in S phase. From 30 µM, the majority of killed cells died in G_2M, the remainder mostly in S phase. Only at the highest concentration more than 10% of killed cells died in G_1.

Discussion

Despite the acknowledged importance of cell cycle events to determine the outcome of a treatment with

Fig. 8 Dose-dependence and time-dependence of the percentage of total (*full height of the bars*) and blocked (*height of the filled areas*) cells in G_1 and in G_2M. This serves to evaluate the impact of the blocking effect on the cell population after treatment with 3, 10, 30, 50, 100 and 300 µM L-PAM. The *error bars* indicate the range where different simulations give predictions fitting the data within the experimental error
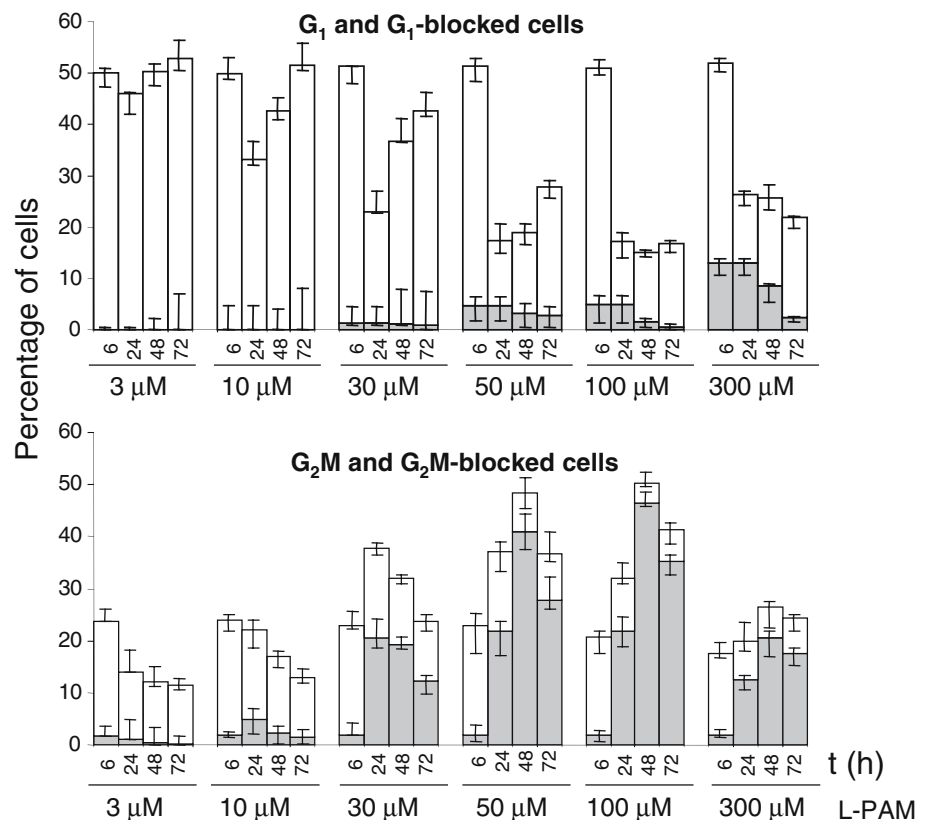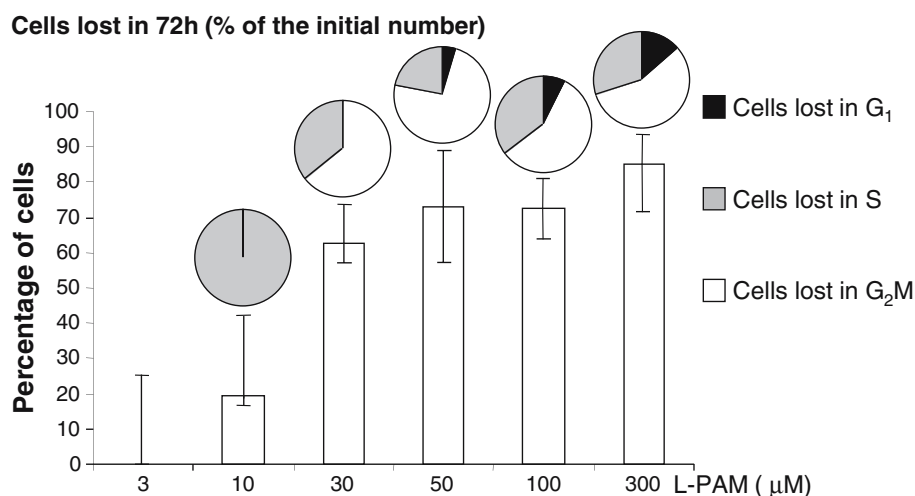
anticancer drugs, classical methods of measuring drug efficacy seem to overlook the complex relationship between cell cycle perturbations and the measured quantity, even at the in vitro level. For instance, an evaluation of growth inhibition, by a colorimetric essay, measures the percentage of absorbance of treated respect to untreated samples at a given -arbitrary- time. The same value can be obtained by blocking cycle progression of all cells without killing them, or by killing a fraction and leaving the other unaffected. More, infinite combinations of a partial cytostatic effect with a partial cytotoxic effect will produce the same measured outcome.

There are methods producing data more oriented to measure cell survival (like a properly performed colony assay) or blocking activity (like DNA flow cytometry); a closer analysis in these cases also reveals that the connection between the number given as "datum" and the underlying phenomenon is not straightforward. For instance, cells blocked for few days and then recovering will not be considered "surviving" if their colony had no time to reach an arbitrarily set threshold size. More badly, the culture (and treatment) conditions required in such assay are often far than optimal for tumour cells, resulting in low plating efficiency. In that respect, an in vitro treatment of an exponentially growing cell population minimises manipulations and potential artefacts. This is the experimental plan adopted in most studies of cell cycle perturbations performed by DNA flow cytometry. But even the interpretation of flow cytometric data is not exempt from ambiguities when more than one cell cycle effect contemporaneously occurs, as it often happens. For instance, no difference may be detected in the DNA profile between well growing untreated cells and another sample treated with drug concentration causing a complete freezing of the cycle. Then, the numerical datum in this case are percentages of cells in G_1, S or G_2M, with the obvious constraint $\%G_1 + \%S + \%G_2M = 100$. That means that a block in a phase or a selective loss in another phase (plus the

usual infinite combinations of both) could cause the same variation of those percentages. Fortunately, in well-designed experiments, replicated flasks are sampled at different times during/after treatment, in the attempt to catch the dynamics of cell cycle perturbations. But the analysis of such sequence of data is not simple. The cell cycle distribution observed at a given time depends on the observation made at the previous time plus the normal cycle flux of cells growing normally, plus the recycling or death of previously blocked cells, plus the result of new blocking or killing activity carried on by checkpoint and apoptotic machinery.

As our intuition easily fell in deciphering this dynamics, we worked on a simulation tool to connect the underlying perturbation scenario, made by blocking and killing activities in G_1, S and G_2M, with the time course of the observed percentages, on the ground of the normal cell cycle flow of unperturbed cells. The mathematical details of the model have been published elsewhere [15]. In the model, each of the cell cycle effects induced by the drug is associated with a single parameter. When different values of each parameter are given as input, the program simulates the consequent cycling of the cell population. Then a comparison is made between the experimental data and the output of the simulation, in order to test the plausibility of the hypotheses based on the input parameters. If we include in the model one parameter-descriptor for each potentially relevant "effect", we have to deal with eight parameters (blocking activity, death rate and recycling in G_1, delay and death rate in S, blocking activity, death rate and recycling in G_2M), each one time- and dose-dependent. As regards S phase, we chose to model an overall reduction of the DNA synthesis rate without a specific compartment for blocked/recycling cells. This choice was coherent with DNA histogram data, which excluded the presence of a specific point in S phase where the cells accumulate. Probably block and recycling are continuous throughout S phase, the result being the average delay rate considered in the model.

The time-dependence was managed by assuming each parameter as constant in each interval between subsequent observations (typically 0–6, 6–24, 24–48 and 48–72 h in our experimental plan). This gives an average effect for each interval.

The experience in using this tool and the ease in recognising the existence of (several) alternative scenarios fully coherent with a time course of %G_1, %S and %G_2M, forced us to reconsider the experimental plan, in the attempt to reach a univocal definition of block and killing dynamics. The first improvement was the parallel measure, at each observation time, of the absolute cell number. In this way, a strong reduction of the possibilities was achieved; however, the existence of differential drug activity for cells treated while in G_1, S or G_2M, was not accounted. Thus, the second experimental improvement was the inclusion of data from pulse-chase BrdUrd experiments, parallel to the doubling of model parameters, to give separate values for the BrdUrd-positive and BrdUrd-negative cell subpopulations. With this analysis, we could determine the cell cycle phase where these subpopulations preferably die, overcoming the problems of synchronisation with chemical or physical agents [10]. Then, we included data from an apoptosis assay (TUNEL), but an analysis of the measuring process convinced us not to rely on the percentage of apoptotic cell detected in this way. In fact, the percentage of dUTP-positive cells detected at a given time depends mainly on the duration of the substage of the apoptotic process where DNA breaks are detectable. Thus, we simply used the TUNEL data as a qualitative assessment of the existence of a killing process ongoing.

The work reported here comes at this stage of development of our project, and is aimed to quantify the response of a cell population in exponential growth to a short L-PAM treatment, distinguishing cytotoxic from cytostatic effects separately within cells that were in S phase at the time of treatment and cells that were in G_1 and G_2M.

By extensively applying a trial-and-error procedure, we started testing scenarios with a few cell cycle perturbations included, adding complexity (i.e. parameters) only when all simpler explanations failed.

As the model was a simplification of the complex cell response to a drug treatment, our aim was not to use it for a precise measure of the parameters but to obtain an estimate of the strength of the corresponding phenomenon, enabling to explain the available data. However, wishing to include all basic perturbations of the cell cycle with their time-dependence, the equations of the model are too complex to be solved and we were not able to obtain cell cycle percentages as analytical functions of those perturbations. For this reason, we made simulations, solving numerically the equations of the model. In this situation, it was not necessary (and also not technically possible in our knowledge) to fit directly the data with some non-linear fitting routine and that we adopted a trial-and-error procedure. This also allowed us to maintain a biological comprehension of the phenomena in all phases of the analysis.

The minimal scenario of parameter values necessary to reproduce all the data (flow cytometric percentages and absolute cell number, plus the qualitative information from dUTP assay) is reported in Fig. 5. This gives a comprehensive description and quantification of the effect of L-PAM in IGROV1 cells, a typical ovarian cancer cell line with wild type p53 whose kinetics features were previously well characterised in our laboratory [5]. The reported scenario is one of the sets of quite similar scenarios explaining all experimental data at the same level of complexity. As demonstrated by the sensitivity analysis, each parameter has a specific range of values within which the simulation reproduces the data within the extent of the experimental error. The sensitivity of each parameter (see Fig. 6) of a cell cycle phase was related to the number of cells flowing or blocked in that phase. If the cells were not flowing into a particular cell cycle phase (e.g. due to total block in the previous phase), we were not able to determine with precision whether cells activated cell cycle controls in that phase. Similarly, if there were only a few cells blocked in a certain phase, we were not able to know their fate, whether they remained blocked, died or recycled. In the analysis of L-PAM, we could not precisely determine the blocking activity in G_1 for BrdUrd-positive cells between 0 and 6 h or the death rate for BrdUrd-positive and BrdUrd-negative cells blocked in G_1. In the other cases, the input parameters were sensitive and gave a coherent description of the time- and dose-dependence of the drug's effects.

The scenario was quite complex, with perturbations in each phase of the cell cycle. For this reason, we addressed the question whether L-PAM acted in a similar way also in other cell lines or this scenario was peculiar for IGROV1 cells. We made similar experiments and analyses using another ovarian carcinoma (A2780) and a colon carcinoma (HCT-116) cell line, and we confirmed most of the features observed with IGROV1 in both the additional cell lines. However, in A2780 cells, the effects were observed at lower drug concentrations, in HCT-116 at higher concentrations respect to IGROV1. This difference of sensitivity amongst the three cell lines might also be caused by events upstream cell cycle response, like different drug transport across cell membrane or different amounts of DNA lesions produced during exposure to L-PAM. The common features characterising cell cycle response to L-PAM treatment in the tested cell lines were the following.

With low concentrations (3 or 10 μM in IGROV1), we detected no effects in G_1, a temporary G_2M block and a more persistent S delay (a weak G_1 block with a shorter S-delay characterized HCT-116 cells). With higher concentrations (≥30 μM in IGROV1), cells in G_1 or in G_2M at the time of treatment were immediately blocked in the same phase. However, G_1 blocking activity was temporary and weak (only 5–20% of cells passing through this phase remained blocked there) while G_2M blocking activity increased with time.

So far as S phase is concerned, our simulation indicated that in the first 24 h there was a net delay (block + recycling) but not loss, while cell loss became evident at longer times after treatment. This suggests that the outcome of S phase block is unbalanced toward repair at short time after treatment, whereas at longer time the cells are more committed to apoptosis. This interpretation is supported by the TUNEL assay (Fig. 4).

Delay S and G_2M block were reported to be an essential step for cells to repair DNA damage [7]. Brox et al. [2] showed that the time at which cells overcome an L-PAM-induced G_2M block correlates with the time when DNA-protein cross-links are removed. In a resistant cell line the DNA interstrand cross-links appeared to be completely repaired in the 48 h after drug removal [9] and at the same time they can recover from G_2M block. Our simulation suggested a G_2M response similar to that in S phase, with a persisting block and cell death after 24 h (intermediate and high L-PAM concentrations) in IGROV1 and A2780 cells, while G_2M cell death was absent in HCT-116. The absence of loss in G_2M represents one of the major differences of the behaviour of HCT-116 cells in respect to IGROV1 and A2780, explaining, at least in part, the lower sensitivity of this cell line. In our analysis, it was necessary to include recycling from G_2M block in order to fit the data of A2780 and HCT-116 cells treated with low L-PAM concentrations, while the fitting of IGROV1 data did not require this parameter but our analysis did not exclude it.

The comparison between the scenarios describing the effects of L-PAM in three different cell lines allowed also to confirm the stronger effects on BrdUrd-negative cells detected with IGROV1, demonstrated by an enrichment of BrdUrd-positive cells (Fig. 3b) in samples treated with intermediate concentrations. The simulation interpreted this phenomenon as especially due to stronger cytostatic effects in S and G_2M in BrdUrd-negative respect to BrdUrd-positive cells, while the relatively higher mortality (in S phase) of BrdUrd-negative cells contributed less to the prevalence of BrdUrd-positive cells at 72 h. At higher concentrations, the effects of the equally strong G_2M block and mortality overwhelmed and limited the differential effect between BrdUrd-negative and BrdUrd-positive cells. This is only partially in agreement with reports using synchronised cells, where subpopulations treated in G_1 or G_2M phase (equivalent to our BrdUrd-negative cells) appeared more sensitive to L-PAM than cells in S phase at the time of treatment [11].

Ludlum suggested that cells alkylated during G_1–S phase might be more sensitive because they have less chance of repairing potentially lethal damage before the next phase of synthesis than in G_2M phase [11]. However, a study of the cell phase-dependent cytotoxicity of nitrogen mustard toward CHO cells concluded that the amount of initial damage and the rate of repair were constant in each phase for this drug [6].

As a whole, our results are not completely in keeping with current paradigms of the effect of L-PAM, pointing to a high level of complexity of the cell response even to simple, short treatments. Moreover, the dose-dependence of the effects was substantial, and a possible explanation to this behaviour could be found in Caporali's study [4]. They demonstrated that the kinetics of activation of several proteins involved in cell cycle checkpoint was strongly dose-dependent. In particular, after a treatment with a low concentration of temozolomide, the activation of ATM was a late event and required a functional MMR system for phosphorylation of Chk1, Chk2 and p53. On the other side, a rapid activation of ATM was detected during treatment with high doses. This dose-dependent behaviour shows also differences during the time after treatment, thus it allows the explanation of the presence of cell cycle effects detected even at long times after treatment. The phenomenon of the presence of long-term effects after short treatment (1 h) with cisplatin was also investigated by Brozovic et al. [3]. In this case, a dose-dependent activation of proteins related with apoptosis was observed even at very long time after treatment (120 h). We also found that cell death was still active at 72 h, but we did not extend our period of observation beyond that time and we were not able to evaluate how long cell death would last.

Moreover, we observed that the percentage of cells lost in 72 h (Fig. 9) reached a sort of plateau for concentrations of L-PAM higher than 30 μM (IGROV1). At lower concentrations, cells were delayed in S and G_2M phases and lethality occurred in S phase. At higher L-PAM concentrations, S and G_2M delay became stronger and more persistent. A cytostatic effect in G_1, without lethality, appeared at these intermediate concentrations. At the highest concentration the lethality in G_1 added to the other effects and the differential response of BrdUrd-positive and BrdUrd-negative cells was definitely lost.

We hope that the deeper understanding of the dynamics of cell cycle response, despite its complexity, would help establishing better rationales for drug scheduling or drug combinations. For instance, the simulation allows an evaluation of the impact of a particular block on the percentage of lost cells. Starting from the scenario describing the effects induced by L-PAM, it was possible to eliminate the delays and blocks at each interval of time (not shown). We found that delay in S phase or G_2M block had no impact on the overall lethality of treatment, and in fact, when one of them was abolished, cells died in the other phase. This means that theoretically, a simple change in a single phase (e.g. by other specific drugs) cannot be expected to improve the treatment [22].

In addition, the loss of phase specificity of the drug at the highest concentration tested and the minimal increase in overall lethality despite a ten-fold increase of the drug concentration (from 30 to 300 μM in our cell line) could be important considerations for cancer treatment.

References

1. Barlogie B, Drewinko B (1977) Lethal and kinetic response of cultured human lymphoid cells to melphalan. Cancer Treat Rep 61:425–436
2. Brox LW, Gowans B, Belch A (1980) L-phenylalanine mustard (melphalan) uptake and cross-linking in the RPMI 6410 human lymphoblastoid cell line. Cancer Res 40:1169–1172
3. Brozovic A, Fritz G, Christmann M, Zisowsky J, Jaehde U, Osmak M, Kaina B (2004) Long-term activation of SAPK/JNK, P38 kinase and FAS-L expression by cisplatin is attenuated in human carcinoma cells that acquired drug resistance. Int J Cancer 112:974–985
4. Caporali S, Falcinelli S, Starace G, Russo MT, Bonmassar E, Jiricny J, D'Atri S (2004) DNA damage induced by temozolomide signals to both ATM and ATR: role of the mismatch repair system. Mol Pharmacol 66:478–491
5. Chiorino G, Metz JA, Tomasoni D, Ubezio P (2001) Desynchronization rate in cell populations: mathematical modeling and experimental data. J Theor Biol 208(2):185–199
6. Clarkson JM, Mitchell DL (1981) The importance of DNA damage and repair in the cell cycle sensitivity of CHO cells to nitrogen mustard. Radiat Res 88:587–596
7. Dean SW, Fox M (1983) Investigation of the cell cycle response of normal and Fanconi's anaemia fibroblasts to nitrogen mustard using flow cytometry. J Cell Sci 64:265–279
8. Erba E, Mascellani E, Pifferi A, D'Incalci M (1995) Comparison of cell-cycle phase perturbations induced by the DNA-minor-groove alkylator tallimustine and by melphalan in the SW626 cell line. Int J Cancer 62:170–175
9. Erickson LC, Osieka R, Kohn KW (1978) Differential repair of 1-(2-chloroethyl)-3-(4-methylcyclohexyl)-1-nitrosourea-induced DNA damage in two human colon tumour cell lines. Cancer Res 38:802–808
10. Linfoot PA, Gray JW, Dean PN, Marton LJ, Deen DF (1986) Effect of cell cycle position on the survival of 9L cells treated with nitrosoureas that alkylate, cross-link, and carbomoylate. Cancer Res 46:2402–2406
11. Ludlum DB (1977) Alkylating agents and the nitrosoureas. In: Becker FF (eds) Cancer, a comprehensive treatise. Plenum Press, New York, pp 285–307
12. Lupi M, Matera G, Branduardi D, D'Incalci M, Ubezio P (2004) Cytostatic and Cytotoxic effects of topotecan decoded by a novel mathematical simulation approach. Cancer Res 64:2825–2832
13. Mattes WB, Hartley JA, Kohn KW (1986) DNA-sequence selectivity of guanine-N7 alkylation by nitrogen mustard. Nucleic Acid Res 14:2971–2987
14. Meyn D, Murray RE (1986) Cell cycle-dependent cytotoxicity of alkylating agents: determination of nitrogen mustard-induced DNA cross-links and their repair in Chinese hamster ovary cells synchronized by centrifugal elutriation. Cancer Res 46:2324–2329
15. Montalenti F, Sena G, Cappella P, Ubezio P (1998) Simulating cancer-cell kinetics after drug treatment: application to cisplatin on ovarian carcinoma. Phys Rev E 57:5877–5887
16. Redwood WR, Colvin M (1980) Transport of melphalan by sensitive and resistant L1210 cells. Cancer Res 40:1144–1149
17. Ross WE, Ewig RAG, Kohn KW (1978) Differences between melphalan and nitrogen mustard in the formation and removal of DNA cross-links. Cancer Res 38:1502–1506
18. Samuels BL, Bitran JD (1995) High-dose intravenous melphalan: a review. J Clin Oncology 13:1786–1799
19. Sarosy G, Leyland-Jones B, Soochan P, Cheson BD (1988) The systemic administration of intravenous melphalan. J Clin Oncol 6:1768–1782
20. Tew KD (1994) Glutathione-associated enzymes in anticancer drug resistance. Cancer Res 54:4313–4320
21. Valeriote F, van Putten L (1975) Proliferation-dependent cytotoxicity of anticancer agents: a review. Cancer Res 35:2619–2630
22. Zhou BS, Bartek J (2004) Targeting the checkpoint kinases: chemosensitization versus chemoprotection. Nat Rev Cancer 4:1–10